10 December 1976, Volume 194, Number 4270 SCIENCE

Variations in the Earth's Orbit: Pacemaker of the Ice Ages

For 500,000 years, major climatic changes have followed variations in obliquity and precession.

J. D. Hays, John Imbrie, N. J. Shackleton

For more than a century the cause of fluctuations in the Pleistocene ice sheets has remained an intriguing and unsolved scientific mystery. Interest in this problem has generated a number of possible explanations (*1*, *2*). One group of theories invokes factors external to the climate system, including variations in the output of the sun, or the amount of solar energy reaching the earth caused by changing concentrations of interstellar dust (*3*); the seasonal and latitudinal distribution of incoming radiation caused by changes in the earth's orbital geometry (*4*); the volcanic dust content of the atmosphere (*5*); and the earth's magnetic field (*6*). Other theories are based on internal elements of the system believed to have response times sufficiently long to yield fluctuations in the range 10^4 to 10^6 years. Such features include the growth and decay of ice sheets (*7*), the surging of the Antarctic ice sheet (*8*); the ice cover of the Arctic Ocean (*9*); the distribution of carbon dioxide between atmosphere and ocean (*10*); and the deep circulation of the ocean (*11*). Additionally, it has been argued that as an almost intransitive system, climate could alternate between different states on an appropriate time scale without the intervention of any external stimulus or internal time constant (*12*).

Among these ideas, only the orbital hypothesis has been formulated so as to predict the frequencies of major Pleistocene glacial fluctuations. Thus it is the only explanation that can be tested geologically by determining what these frequencies are. Our main purpose here is to make such a test.

Previous work has provided strong suggestive evidence that orbital changes induced climatic change (*13–20*). However, two primary obstacles have led to continuing controversy. The first is the uncertainty in identifying which aspects of the radiation budget are critical to climatic change. Depending on the latitude and season considered most significant, grossly different climatic records can be predicted from the same astronomical data. Milankovitch (*4*) followed Koppen and Wegener's (*21*) view that the distribution of summer insolation (solar radiation received at the top of the atmosphere) at 65°N should be critical to the growth and decay of ice sheets. Hence the curve of summer insolation at this latitude has been taken by many as a prediction of the world climate curve. Kukla (*19*) has pointed out weaknesses in Koppen and Wegener's proposal and has suggested that the critical time may be September and October in both hemispheres. However, several other curves have been supported by plausible arguments. As a result, dates estimated for the last interglacial on the basis of these curves have ranged from 80,000 to 180,000 years ago (*22*).

The second and more critical problem in testing the orbital theory has been the uncertainty of geological chronology. Until recently the inaccuracy of dating methods limited the interval over which a meaningful test could be made to the last 150,000 years. Hence the most convincing arguments advanced in support of the orbital theory to date have been based on the ages of 80,000, 105,000, and 125,000 years obtained for coral terraces first on Barbados (*15*) and later on New Guinea (*23*) and Hawaii (*24*). These structures record episodes of high sea level (and therefore low ice volume) at times predicted by the Milankovitch theory. Unfortunately, dates for older terraces are too uncertain to yield a definitive test (*25*).

More climatic information is provided by the continuous records from deep-sea cores, especially the oxygen isotope record obtained by Emiliani (*26*). However, the quasi-periodic nature of both the isotopic and insolation curves, and the uncertain chronology of the older geologic records, have combined to render plausible different astronomical interpretations of the same geologic data (*13*, *14*, *17*, *27*).

Strategy

All versions of the orbital hypothesis of climatic change predict that the obliquity of the earth's axis (with a period of about 41,000 years) and the precession of the equinoxes (period of about 21,000 years) are the underlying, controlling variables that influence climate through their impact on planetary insolation. Most of these hypotheses single out

The authors are all members of the CLIMAP project. J. D. Hays is professor of geology at Columbia University, New York 10027, and is on the staff of the Lamont-Doherty Geological Observatory, Palisades, New York 10964. John Imbrie is Henry L. Doherty professor of oceanography, Brown University, Providence, Rhode Island 02912. N. J. Shackleton is on the staff of the Sub-department of Quaternary Research, Cambridge University, Cambridge, England.

mechanisms of climatic change which are presumed to respond to particular elements in the insolation regime (*28*). In our more generalized version of the hypothesis we treat secular changes in the orbit as a forcing function of a system whose output is the geological record of climate—without identifying or evaluating the mechanisms through which climate is modified by changes in the global pattern of incoming radiation (*29*). Most of our climatic analysis is based on the simplifying assumption that the climate system responds linearly to orbital forcing. The consequences of a more realistic, nonlinear response are examined in a final section here.

Our geological data comprise measurements of three climatically sensitive parameters in two deep-sea sediment cores. These cores were taken from an area where previous work shows that sediment is accumulating fast enough to preserve information at the frequencies of interest. Measurements of one variable, the per mil enrichment of oxygen-18 ($\delta^{18}O$), make it possible to correlate these records with others throughout the world, and to establish that the sediment studied accumulated without significant hiatuses and at rates which show no major fluctuations.

To be used in tests of the orbital hypothesis, these data are transformed into geological time series. In our first test we make the simplest geochronological assumption, that sediment accumulated in each core at a constant rate throughout the period of study. Later we relax this assumption and allow slight changes in accumulation rate, as indicated by additional geochronological data.

Our frequency-domain tests use the numerical techniques of spectral analysis and are designed to seek evidence for a concentration of spectral energy at the frequencies of variation in obliquity and precession. We consider that support for the hypothesis can be decisive if both frequencies are detected and, to allow for geochronological uncertainties, if it can be clearly demonstrated that the ratio of the two frequencies detected does not differ significantly from the predicted ratio (about 1.8).

Finally, our time-domain tests are designed to examine the phase coherence between the three climatic records and between each record and the postulated forcing function. To this end we use the numerical techniques of bandpass filter analysis. Such an approach makes it possible to examine separately the variance components of the geological records that correspond in frequency to the variations of obliquity and precession.

Methods

Core selection. From several hundred cores studied stratigraphically by the CLIMAP project, we selected two (RC11-120 and E49-18) whose locations (Fig. 1 and Table 1) and properties make them ideal for testing the orbital hypothesis. Most important, they contain together a climatic record that is continuous, long enough to be statistically useful (450,000 years), and characterized by accumulation rates fast enough (> 3 centimeters per 1,000 years) to resolve climatic fluctuations with periods well below 20,000 years. In addition, the cores are centrally located between Africa, Australia, and Antarctica, and therefore little influenced by variations of erosional detritus from these continents. Finally, as explained below, a Southern Hemisphere location provides an opportunity to monitor simultaneously both Northern Hemisphere ice volume and Southern Hemisphere temperature. No other cores known to us have all these attributes.

Geological data. We have measured (i) $\delta^{18}O$, the oxygen isotopic composition of planktonic foraminifera; (ii) *Ts*, an estimate of summer sea-surface temperatures at the core site, derived from a statistical analysis of radiolarian assemblages; and (iii) percentage of *Cycladophora davisiana*, the relative abundance of a radiolarian species not used in the estimation of *Ts*. Identical samples were analyzed for the three variables at 10-cm intervals through each core (*30*).

Oxygen isotope analyses have been made in tests of *Globigerina bulloides* by well-established techniques (*31, 32*). The reproducibility for independent samples from the sediment is about ± 0.1 per mil [1 standard deviation (S.D.)]. Tests of *G. bulloides* are formed primarily at some depth below the sea surface so that changes in surface temperature do not greatly affect the temperature at which the carbonate is secreted. Down-core variations in $\delta^{18}O$ reflect changes in oceanic isotopic composition, caused primarily by the waxing and waning of Northern Hemisphere ice sheets (*31, 33*). Thus, the $\delta^{18}O$ in our subantarctic cores is a Northern Hemisphere climatic record.

Estimates of *Ts* were made by applying statistical techniques (*18*) to subantarctic radiolarians. The data base for writing the transfer functions has been expanded from that of Lozano and Hays (*34*) by G. Irving and J. Morley to include cores in the vicinity of E49-18. The accuracy of *Ts* as an estimate of sea-surface temperature is ± 1.5°C; its reproducibility as an index of faunal change is ± 0.32°C (1 S.D.).

The percentage of *C. davisiana* relative to all other radiolarians was determined by techniques previously described (*35*). These counts have a precision of about ± 0.74 percent (1 S.D.). The recent distribution of the cosmopolitan species *C. davisiana* Petrushevskaya shows no relation to present sea-surface temperature (*34, 36*), so that the remarkable Pleistocene abundance variations of this species (which comprised up to 50 percent of the fauna during glacial maxima in some areas) are also probably not due to temperature (*35*). The unique high abundance of this species in recent sediments of the Sea of Okhotsk has been related to the structure of summer surface waters, where a low-salinity surface layer is underlain by a strong temperature minimum (*37*). The high abundance of *C. davisiana* during glacial times in the Antarctic may be due to a similar surface water structure.

Measurements of these parameters therefore reflect changes in three parts of the climate system: Northern Hemisphere land ice, subantarctic sea-surface temperature, and Antarctic surface water structure.

Orbital data. Since the pioneering work of Milankovitch (*4*) the chronologies for orbital and insolation changes have been recalculated several times (*38–40*). These papers and those of Kukla (*19*) should be consulted for an explanation and evaluation of the numerical procedures used and for a discussion of the manner in which orbital changes bear on the earth's insolation regime as a function of latitude, season, and time.

Table 1. Core locations and depths.

Core	Length (cm)	Water depth (m)	Latitude	Longitude
RC11-120	954	3135	43°31′S	79°52′E
E49-18	1459	3256	46°03′S	90°09′E

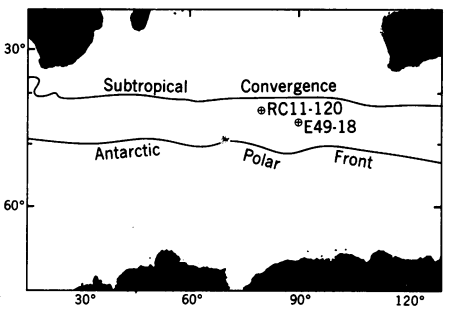

Fig. 1. Locations of cores in the southern Indian Ocean.

When Vernekar's (*39*) calculations are compared with those of Berger (*40*), the timing of inflection points in the obliquity and precession curves do not differ by more than 1000 years over the past 400,000 years. For intervals older than 500,000 years ago, however, discrepancies between the calculations become significant, and the work of Berger is to be preferred because it includes the effect of higher-order terms.

Geological Time Series

Stratigraphic sequence. Because the $\delta^{18}O$ record in deep-sea sediments primarily reflects global ice volume, it is globally synchronous in open-ocean cores and provides (along with standard biostratigraphical techniques) a basic stratigraphy for the last million years (*33, 41, 42*). This stratigraphy has a resolution limited only by ocean mixing (about 1000 years) and bioturbation. The $\delta^{18}O$ record was divided by Emiliani (*26*) into numbered stratigraphic stages, which are used here.

The oxygen isotope record in core RC11-120 is complete and typical back to late stage 9 (Fig. 2). Stage 5 shows its characteristic three peaks (*26, 42*); and stage 7 is interrupted by a sharp positive excursion, which is typical (*31, 42*).

In core E49-18 (Fig. 3) the high percentage of *C. davisiana* at the top indicates that the Holocene is missing (*35*); the top may be as old as 60,000 years. In addition, visual inspection of the core shows that it has been mechanically stretched between 300 and 400 cm during the coring process. Consequently, the core was analyzed for $\delta^{18}O$ only from the lower part of stage 5 to the base. The record of stages 6 to 9 is similar to the equivalent part of core RC11-120; the remainder can be compared stage by stage with other cores (*31, 42*). As in other cores studied, stage 12 is bracketed by the extinction of the coccolith *Pseudoemiliania lacunosa* below (*43*) and the radiolarian *Stylatractus universus* above (*44*). This confirms the presence of the entire oxygen isotope sequence from stage 6 to stage 13.

The *Ts* curve in both cores differs markedly in shape from the $\delta^{18}O$ curve, being characterized by abrupt increases of estimated temperature of up to 6°C in stage 1 and at the base of stages 5, 7, 9, and 11. Elsewhere in the cores *Ts* fluctuations do not exceed 3°C. The spiky character of this record is similar to that of certain Atlantic cores from high northern latitudes (*45*).

Above stage 10 there is near synchroneity between the $\delta^{18}O$ minima and *Ts* maxima. However, changes in *Ts* precede changes in $\delta^{18}O$ by a small amount; this is most evident at extreme *Ts* maxima. We conclude that over this time interval changes in Northern Hemisphere ice volume and subantarctic sea-surface temperature are nearly synchronous. Between stage 10 and the upper part of stage 11, however, the higher-frequency fluctuations in *Ts* and $\delta^{18}O$ appear to be out of phase; and the low-temperature extremes are colder than they are at higher levels in the cores.

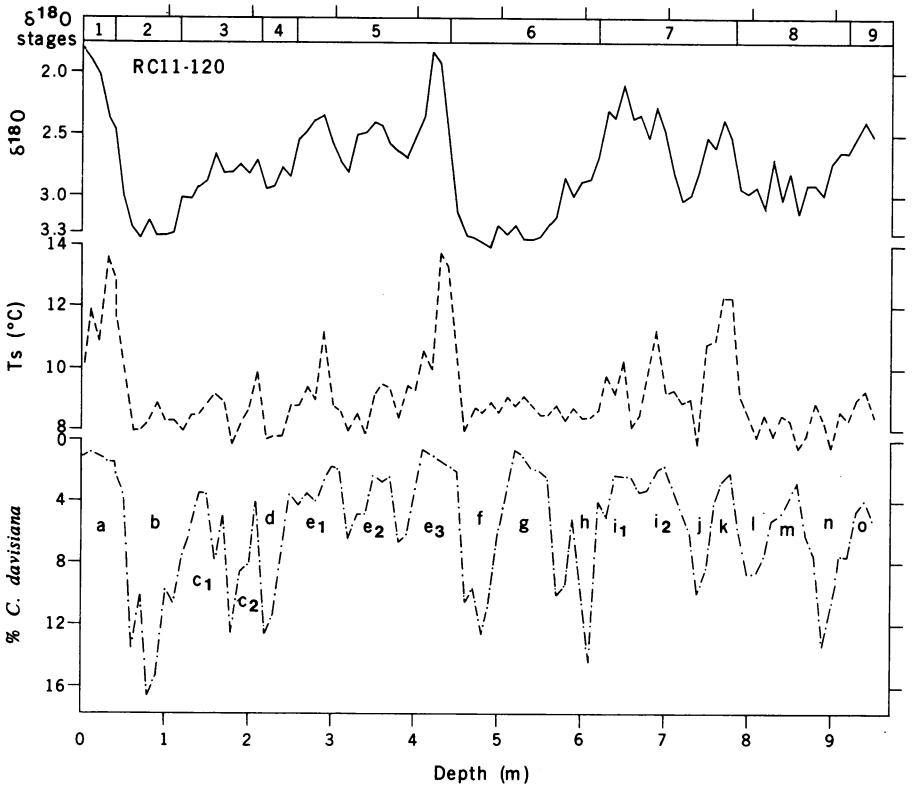

Fig. 2. Depth plots of three parameters measured in core RC11-120: $\delta^{18}O$ (solid line), *Ts* (dashed line), and percentage of *C. davisiana* (dash-dot line). Letter designations of peaks on the latter curve are informal designations of various parts of the record.

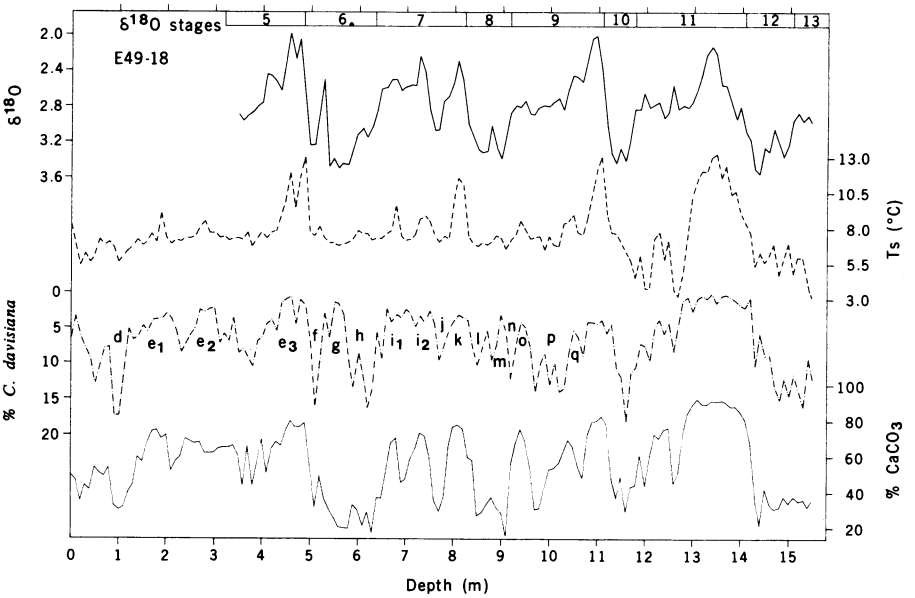

Fig. 3. Depth plots of four parameters measured in core E49-18: $\delta^{18}O$ (solid line at the top), *Ts* (dashed line), percentage of *C. davisiana* (dash-dot line), and percentage of $CaCO_3$ (solid line at the bottom). The technique used for $CaCO_3$ measurement is that of Hülsemann (*81*). A comparison of the lettered intervals of the *C. davisiana* curve for this core with those for core RC11-120 (Fig. 2) shows that the time represented by the top 1.5 m of RC11-120 is not present in E49-18.

Table 2. Chronologic assumptions of age models. Interpolation within and extrapolation beyond control points shown is linear. For the combined PATCH ELBOW and PATCH TUNE-UP records, data from 0 to 785 cm in RC11-120 were combined with data below 825 cm in E49-18.

Age model	Core	Depth (cm)	Age ($\times 10^3$ years)	Sedimentation rate (cm/10^3 years)
SIMPLEX	RC11-120	0	0	3.46
		440	127*	
	E49-18	490	127*	2.92
		1405	440†	
ELBOW	RC11-120	0	0	
		39	9.4‡	4.14
		440	127*	3.40
		785	251†	2.78
	E49-18	490	127*	
		825	251†	2.70
		1405	440†	3.06
TUNE-UP	RC11-120	0	0	
		39	9.4‡	4.14
		440	127*	3.40
		785	247	2.87
	E49-18	490	127*	
		825	247	2.79
		1405	425	3.26

*Age of isotopic stage 6–5 boundary (*17*). †Age of isotopic stage 8–7 boundary (251,000 years) and boundary 12–11 (440,000 years) (*31*). ‡Carbon-14 determination (*35*).

Table 3. Frequency-domain test of orbital theory based on SIMPLEX chronology for two deep-sea cores. Values are mean periods (in thousand years per cycle) of peaks in unprewhitened geologic and orbital spectra.

Geologic data						Orbital data	
Core	Time interval ($\times 10^3$ B.P.)	Frequency band	*Ts*	$\delta^{18}O$	*C. davisiana* (%)	Spectral estimate	Element
RC11-120	0–273*	*a*	87	91	106		
		b	38	38	37	40.8	Obliquity (ϵ)
		c	21	23		22.6	Precession (P)
		b/c	1.8	1.7		1.8	ϵ/P
E49-18	127–489†	*a*	94	109	119		
		b	43	47		41.1	Obliquity (ϵ)
		c	24	24		21.9	Precession (P)
		b/c	1.8	1.9		1.9	ϵ/P

*Geologic and orbital spectra for this interval were calculated with $n = 91$ and $m = 40$ (*57*). †Geologic and orbital spectra for this interval were calculated with $n = 121$ and $m = 50$ (*57*).

Table 4. Frequency-domain test of orbital theory using ELBOW chronology for PATCH core. Values are mean periods (in thousand years per cycle) of peaks and subpeaks in geologic and orbital spectra [$n = 163$ and $m = 50$ (*57*)]. Orbital data calculations cover the past 468,000 years.

Frequency band	Geologic data						Orbital data		
	Unprewhitened spectra			Prewhitened spectra					
	Ts	$\delta^{18}O$	*C. davisiana* (%)	*Ts*	$\delta^{18}O$	*C. davisiana* (%)	Spectral estimate	Time domain estimate	Element
a	94	106	122				105	97	Eccentricity (e)
b	40	43	43	42	43*	42*	41.1	40.6	Obliquity (ϵ)
c_1	23	24	24	24*	24	24	23.1		Precession (P_1)
c_m				22*	22	22	21.8	21.6	Precession (P_m)
c_2		19.5		19.5	19.5	19.5	18.8		Precession (P_2)
b/c_1	1.7	1.8	1.8	1.8	1.8	1.7	1.78		ϵ/P_1

*Peaks in prewhitened spectra are significant at $P = .05$.

Although the percentage *C. davisiana* curve has a character distinct from the other two, its maxima are generally correlated in timing, but not in amplitude, with *Ts* minima and $\delta^{18}O$ maxima, except in stages 8 and 9.

Time control. A basic chronological framework for these sequences is established by determining the absolute ages of certain horizons. In RC11-120, carbon-14 dating at the 36- to 39-cm level yields an age of 9400 ± 600 years (*35*). This level marks the most recent *Ts* maximum and substantially precedes the Northern Hemisphere hypsithermal, which at many sites has been dated at about 6000 years ago (*1*).

The age of the boundary between stage 12 and stage 11 was taken from Shackleton and Opdyke (*31*), who estimated it at 440,000 years in an equatorial Pacific core (V28-238) by assuming uniform accumulation between the core top and the magnetic reversal marking the Brunhes-Matuyama boundary. Extinction of *S. universus* occurred globally on this stage boundary (*44*), so that the estimates of 400,000 years for the age of this extinction (*46*) in the North Pacific and Antarctic constitute independent determinations for the age of the 12-11 boundary. The range of these figures expresses the current age uncertainty of this boundary (*47*).

In many areas there is evidence for a change in accumulation rate around stage 6 (*48*) so that we have used an independent estimate of 251,000 years for the stage 8-7 boundary. This estimate, like that for the 12-11 boundary, was taken from Pacific core V28-238 (*31*).

The age of the stage 6-5 boundary is within the range of several radiometric dating techniques, and has been the cornerstone of some previous attempts to support specific versions of the orbital hypothesis. We have used an age of 127,000 years which has an analytical error estimated at ± 6000 years (*17*). At this point in our analysis we do not experiment with other published ages (*49*) because it is very difficult to reconcile all the terrace coral ages from Barbados, New Guinea, and Hawaii (*15, 23, 24, 50*) and data from deep-sea cores (*51*) with any substantially different age (*52*).

Chronological models. To test the orbital theory, age models (Table 2) must be developed to express each geological variable as a function of time. We do this by assuming that sediment accumulated at a constant rate between the horizons for which we have independent estimates of age. Although uniform sedimentation is an ideal which is unlikely to prevail precisely anywhere, the fact that

the characteristics of the oxygen isotope record are present throughout the cores suggests that there can be no substantial lacunae, while the striking resemblance to records from distant areas shows that there can be no gross distortions of accumulation rate.

SIMPLEX models assume uniform sedimentation rates through each core and fix the core top of RC11-120 at zero, the 6-5 stage boundary at 127,000 years (cores RC11-120 and E49-18), and the 12-11 stage boundary at 440,000 years (core E49-18; see Table 2). It is important to note that although the SIMPLEX model presents each variable as a function of age, the age estimated is an exact linear function of depth in the core.

ELBOW models use more chronological information and no longer represent the records as a simple function of depth (Table 2). Sedimentation rates change slightly at three control points and are assumed constant between them.

PATCH is a time series in which we have joined the records of the two cores at the 8-7 stage boundary, thereby providing a longer and statistically more useful record. Another model in which the cores were joined at the 6-5 stage boundary was found to be statistically almost identical and is not considered here.

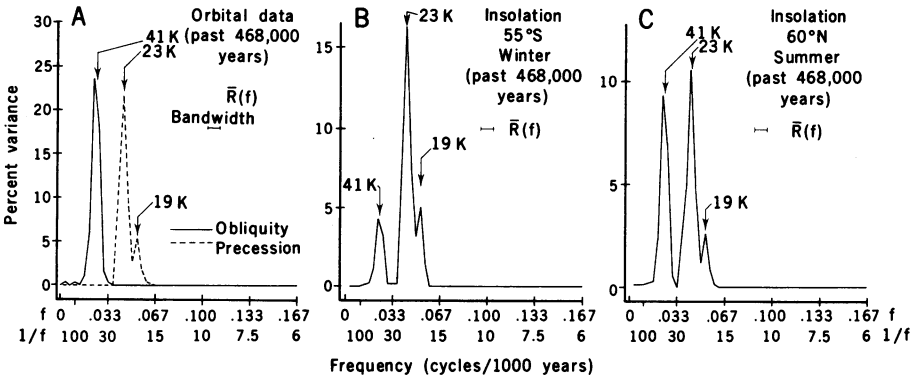

Fig. 4. High-resolution spectra of orbital and insolation variations over the past 468,000 years. Variance (as percentage of total variance per unit frequency band) is plotted as a function of frequency (cycles per thousand years). Arrows indicate weighted mean cycle lengths of spectral peaks (in thousands of years). (A) Spectra for obliquity and precession ($\Delta e \sin\Pi$). (B) Spectrum for winter insolation at 55°S. (C) Spectrum for summer insolation at 60°N. [All data are from Vernekar (*39*)]

Frequency-Domain Tests

Assumptions. From the viewpoint of linear-systems modeling (*53*) the astronomical theory of Milankovitch postulates two systems operating in series. The first is a radiation system which transforms orbital signals (obliquity and precession) into a set of insolation signals (one for each combination of latitude and season). The insolation signals are transformed by a second, explicitly formulated climate-response system into (predicted) climate curves. In contrast, we postulate a single, radiation-climate system which transforms orbital inputs into climatic outputs. We can therefore avoid the obligation of identifying the physical mechanisms of climatic response and specify the behavior of the system only in general terms (*54*). The dynamics of our model are fixed by assuming that the system is a time-invariant, linear system—that is, that its behavior in the time domain can be described by a linear differential equation with constant coefficients. The response of such a system in the frequency domain is well known: frequencies in the output match those of the input, but their amplitudes are modulated at different frequencies according to a gain function (*55*). Therefore, whatever frequencies characterize the orbital signals, we will expect to find them emphasized in paleoclimatic spectra (except for frequencies so high that they would be greatly attenuated by the time constants of response).

Numerical procedures. The statistical techniques we use to calculate both orbital and climatic spectra are taken without modification from the work of Blackman and Tukey (*56*) with elaborations by Jenkins and Watts (*55*). Our procedure involves ten sequential steps: selection of an absolute chronology, calculation of a time series, detrending, prewhitening (optional), lagging, calculation of the autocovariance function, smoothing with a Hamming lag window, spectral estimation, scaling, and statistical evaluation (*57, 58*). In all calculations the sampling interval is fixed at 3000 years; hence the spectral estimates cover a frequency band ranging up to the Nyquist frequency of 0.167 cycle per thousand years.

Frequency analysis of astronomical data. For any particular latitude the intensity of solar radiation received at the top of the atmosphere varies quasi-periodically with three elements of the earth's orbit: eccentricity, obliquity, and the longitude of perihelion based on the moving equinox. Over the last 4 million years the eccentricity (e, the ratio of the focal distance to the length of the major axis) ranges from a value near zero to a maximum of about 0.06, and exhibits an average period of 93,000 years (*39*). Variations in e, unlike variations in the other orbital elements, also slightly affect the total annual insolation received by the earth. Because the extreme range of this effect over the past 500,000 years is about 0.1 percent, it has generally been considered unimportant (*59*). Obliquity (ϵ, the angle between the equatorial and ecliptic planes) ranges from 22.1° to 24.5°, with an average period of about 41,000 years (*39*).

The climatic effect of precession is a function of Π, the longitude of perihelion based on the moving equinox, and e (*60*). Specifically, the intensity of incoming solar radiation at a particular latitude and season varies as $e\sin\Pi$. To express these variations as a time series, the value of $e\sin\Pi$ for June 1950 A.D. is subtracted from the same quantity calculated for particular times in the past. The resulting precessional index ($\Delta e \sin\Pi$) is approximately equal to the deviation from its 1950 value of the earth-sun distance in June, expressed as a fraction of the semi-major axis of the earth's orbit (*61*). Over the past 4 million years, this index ranges from about +0.03 to −0.07 and has an average period of about 21,000 years (*39*).

We have used spectral techniques to analyze secular variations in ϵ, e, $\sin\Pi$, and $\Delta e \sin\Pi$ (*62*). Because these variations are quasi-periodic, it is necessary to specify the interval over which frequencies are to be analyzed (*63*); our analyses (Tables 3 and 4 and Fig. 4) treat time intervals corresponding to the core records.

Spectra calculated for variations in eccentricity and obliquity over the past 468,000 years (Table 4) are both unimodal; that is, they have spectral peaks dominated by a single frequency (*64*). These spectral peaks correspond to cycles of 105,000 years (eccentricity) and 41,000 years (obliquity). Spectra calculated for $\sin\Pi$ (not tabulated) and for $\Delta e \sin\Pi$ are more complex. Both are bimodal, with subpeaks corresponding to cycles of 23,000 years (P_1) and 19,000 years (P_2).

We have also calculated spectra for two time series recording variations in insolation (Fig. 4), one for 55°S and the other for 60°N (*39*). To the nearest 1000 years, the three dominant cycles in these spectra (41,000, 23,000, and 19,000 years) correspond to those observed in the spectra for obliquity and precession. This result, although expected, underscores two important points. First, insolation spectra are characterized by frequencies reflecting obliquity and precession, but not eccentricity. Second, the relative importance of the insolation components due to obliquity and precession varies with latitude and season.

Frequency analysis of geological data. Using techniques identical to those applied to the astronomical data, we have calculated spectra for each of the three geological variables: *Ts*, $\delta^{18}O$, and percentage of *C. davisiana* (Fig. 5). The SIMPLEX chronology is used to analyze the individual cores, and the ELBOW chronology is applied to the combined (PATCH) core.

Because the SIMPLEX time series are undesirably short and are based on limited chronological control, we do not place much reliance on the accuracy of estimates of their constituent frequencies. Nevertheless, five of the six spectra calculated are characterized by three discrete peaks, which occupy the same parts of the frequency range in each spectrum (Table 3). Those corresponding to periods from 87,000 to 119,000 years are labeled *a*; 37,000 to 47,000 years *b*; and 21,000 to 24,000 years *c*. This suggests that the *b* and *c* peaks represent a response to obliquity and precession variation, respectively.

The ratios of obliquity period to precession period calculated for the intervals of time covered by cores RC11-120 and E49-18 are 1.8 and 1.9, respectively (Table 3). The observed ratios of the dominant period in peak *b* to the dominant period in peak *c* are 1.7 ± 0.1 and 1.9 ± 0.1 for RC11-120 and E49-18, respectively. Because the observed ratios from these geological data are independent of the ages used to calibrate the SIMPLEX time series and closely match ratios derived for orbital data, we conclude that the ratio test supports the hypothesis of orbital control.

To obtain accurate estimates of the climatic frequencies, we now examine spectra calculated from ELBOW time series for the combined (PATCH) time series. As before, the climatic variance is distributed mainly in three discrete spectral peaks (Table 4 and Fig. 5). More than half of the total variance is contained in the low-frequency *a* peak (62 percent for *Ts*, 58 percent for $\delta^{18}O$, and 51 percent for *C. davisiana*). All three peaks are unimodal. Estimates of the dominant cycle in the *a* peaks are 94,000, 106,000, and 122,000 years for *Ts*, $\delta^{18}O$, and percentage of *C. davisiana*, respectively. Because these estimates are derived from the low-frequency end of the spectrum, they should be regarded as rough estimates. However, there can be no doubt that a spectral peak centered near a 100,000-year cycle is a major feature of the climatic record.

A substantial fraction of the variance is contained in the *b* peaks: 19 percent for *Ts*, 27 percent for $\delta^{18}O$, and 30 percent for *C. davisiana* (Fig. 5). Each of the three peaks is unimodal. Estimates of this dominant cycle in the peaks range from 40,000 to 43,000 years (Table 3).

A smaller fraction of the total variance is contained in the *c* peaks: 11 percent for *Ts*, 9 percent for $\delta^{18}O$, and 7 percent for *C. davisiana*. The *Ts* and *C. davisiana* peaks, both unimodal, correspond to cycles of 23,000 and 24,000 years, respectively (Table 4). The *c* peak in the $\delta^{18}O$ spectrum is bimodal, with subpeaks (c_1 and c_2) corresponding to cycles of 24,000 and 19,500 years (Table 4).

Although the statistical significance of the *a* peaks can hardly be in doubt, for peaks *b* and *c* a more detailed examination and statistical evaluation are clearly desirable. These objectives are achieved by expressing the variance on a log scale (Fig. 6, top) and by prewhitening the signal to reduce distortions in the higher-frequency part of the spectrum caused by variance transfer from the *a* peak during analysis. The resulting spectra, which have the flat trend desired (Fig. 6, bottom), should be used in the higher-frequency part of the spectrum, not only to conduct statistical tests but also to obtain more accurate frequency estimates.

Estimates of *b* peak frequencies in the prewhitened signals are changed very little; their dominant cycles now range from 42,000 to 43,000 years (Table 4). The *c* peaks differ mainly in the appearance of a small subsidiary peak in the *Ts* spectrum. The midpoints of the three c_1 peaks now correspond to cycles 24,000 years long; and the midpoints of the c_2 peaks in the *Ts* and $\delta^{18}O$ spectra correspond to a 19,500-year cycle (Fig. 6 and Table 4).

Statistical evaluation. Based on the

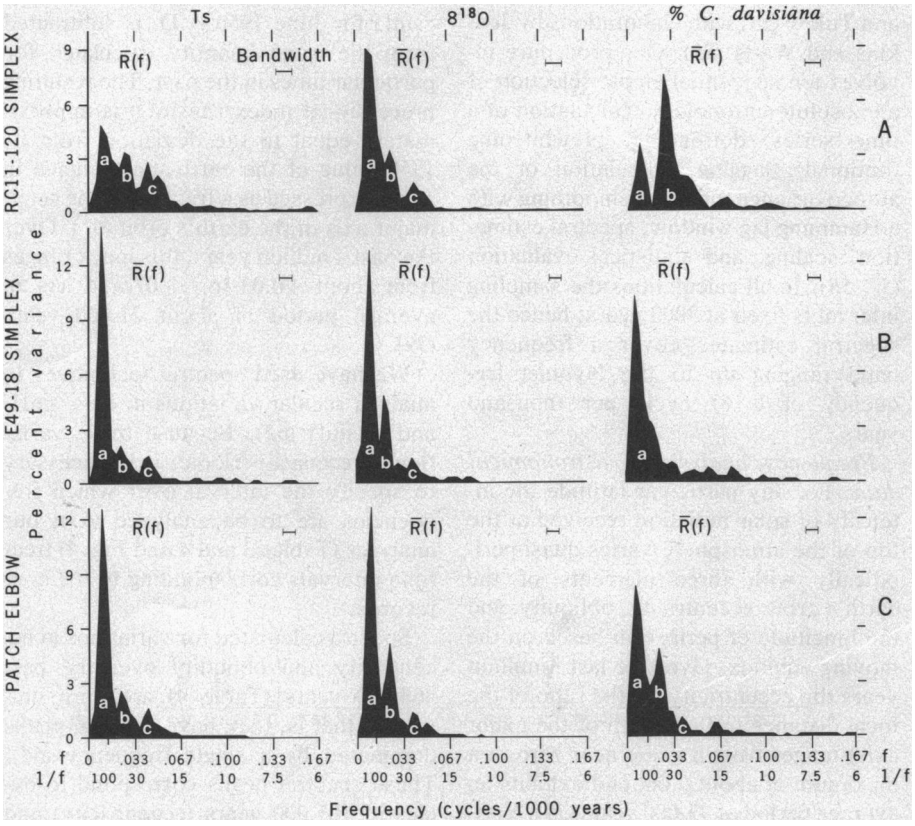

Fig. 5. High-resolution spectra of climatic variations in *Ts*, $\delta^{18}O$, and percentage of *C. davisiana*. Variance (as percentage of total variance per unit frequency band) is plotted as a function of frequency (cycles per thousand years). Prominent spectral peaks are labeled *a*, *b*, and *c*. Arrows indicate weighted mean cycle lengths (in thousands of years). The age models used in the calculations are given in Table 2. (A) Spectra for core RC11-120 are calculated for the SIMPLEX age model. (B) Spectra for core E49-18 are calculated for the SIMPLEX age model. (C) Spectra of the combined (PATCH) record are calculated for the ELBOW age model.

null hypothesis that the data are a sample of a random signal having a general distribution of variance like that in the observed low-resolution spectrum, confidence intervals are calculated as a guide to the statistical significance of spectral estimates in the high-resolution spectrum (Fig. 6). A particular peak in that spectrum is judged significant if it extends above the low-resolution spectrum by an amount that exceeds the appropriate one-sided confidence interval. Of the three *b* peaks, one is significant at $P = .02$ (*C. davisiana*) and one at $P = .05$ ($\delta^{18}O$). Of the three c_1 peaks, one (*Ts*) is significant at $P = .05$ (*65*).

We carefully considered aliasing and harmonic problems (*66*) and conclude that our spectral peaks are not an artifact of procedure. This conclusion was supported by examining more detailed spectra calculated by the maximum entropy technique (*67*).

Discussion. Having examined the confidence intervals for individual climatic spectra, and having eliminated the aliasing and harmonic problems, we can now ask if the frequencies found in the three spectra are those predicted by our linear version of orbital theory. In making this frequency-domain test we must note that the geologic spectra contain substantial variance components at many frequencies in the range of interest, and not simply ask whether there are statistically significant frequencies which match those predicted but whether the spectra observed show sufficient emphasis at the frequencies predicted to be accepted as nonrandom results (*65*). Our answer is "yes" for the following reasons: (i) Using a chronology that is completely independent of the astronomical theory, we find that modal frequencies observed in the geological record match the obliquity and precession frequencies to within 5 percent. The coherence of these results across different variables measured in two cores we regard as very powerful support for the theory. (ii) Two geological spectra ($\delta^{18}O$ and percentage of *C. davisiana*) have peaks corresponding to the predicted obliquity frequency that are significant at $P = .05$. One geological spectrum (*Ts*) has a peak corresponding to the dominant precession frequency which is also significant at $P = .05$. (iii) In addition, the predicted ratios of obliquity to precession frequencies (calculated for the time intervals represented by cores RC11-120 and E49-18) match the ratios of measured climatic frequencies in the two cores (using the SIMPLEX chronology) to within 5 percent—a result that is independent of absolute age specifications and depends only on the assumption of constant accumulation rates.

Having found the frequencies of obliquity and precession in our geological records—as predicted by a linear version of the theory of orbital control—we should consider again the lower-frequency climatic components which, although not predicted, actually contain about half of the observed variance. These components form the *a* peaks in our spectra. Concentrated at periods near 100,000 years (Figs. 5 and 6), they are close to the 105,000-year period in the eccentricity spectrum (Table 4). This similarity of the dominant frequencies in late Quaternary records of climate and eccentricity has been noted before (*13, 17, 18*) and demands an explanation. One hypothesis (developed further below) is that the radiation-climate system responds nonlinearly (*68*) to changes in the geographic and seasonal distribution of insolation. Another is that the small control eccentricity exerts on the total annual insolation is significant climatically (*59*).

An apparently independent confirmation of our conclusions about spectral peaks *b* and *c* can be found in reports of climatic periodicities in the $\delta^{18}O$ record closely matching those of obliquity and precession (*14, 16, 20, 26, 69*). However, the time scale used in these investigations differs from ours by about a factor of 2. The explanation of this paradox is to be found in the dominant climatic periodicity, which in all of the cores is the 100,000-year cycle, and not, as expected (*2, 26*), the geologic response to the 41,000-year obliquity cycle (Table 5). The spectral peak identified by Kemp and Eger (*16*) and by Chappell (*20*) as due to precession, corresponds to our *b* peak, and therefore (we argue) is actually an effect of obliquity. The spectral peak identified by van den Huevel (*14*) as due to the precession half-cycle corresponds to our *c* peak, and therefore is now to be understood as the effect of a full precession cycle. Only with the advent of chronologies based on the Brunhes-Matuyama magnetic reversal (*17, 18, 31*) was the dominant climatic period in the $\delta^{18}O$ record identified as approximately 100,000 years (Table 5).

Time-Domain Tests

Assumptions. As with the frequency-domain test, we start here with the assumption that the radiation-climate system is time-invariant and linear. One well-known characteristic of such a system forms the basis for our time-domain tests: any frequency component of the

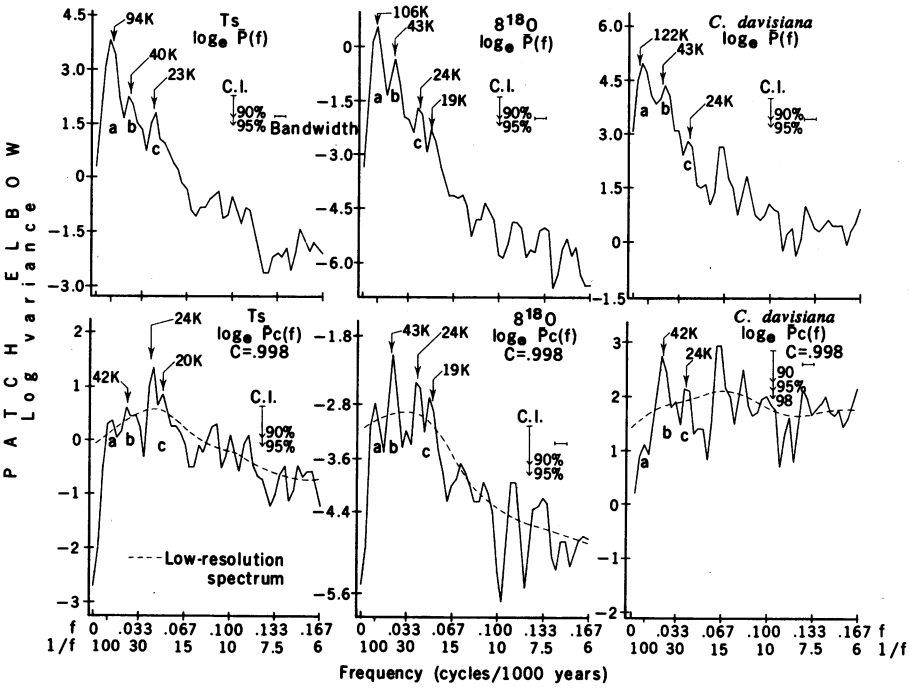

Fig. 6. Spectra of climatic variations (in *Ts*, $\delta^{18}O$, and percentage of *C. davisiana*) in the combined (PATCH) record from two subantarctic deep-sea cores. Calculations are based on the ELBOW age model (Table 2). Arrows without crossbars indicate weighted mean cycle lengths of spectral peaks (in thousands of years). Arrows with crossbars show one-sided confidence intervals (*C.I.*) attached to estimates in the high-resolution spectrum. Prominent spectral peaks are labeled *a*, *b*, and *c*. (Top row) High-resolution spectra from Fig. 5C expressed as the natural log of the variance as a function of frequency (cycles per thousand years). (Bottom row) High-resolution spectra (solid line) and low-resolution spectra (dashed line) after prewhitening with a first-difference filter.

input signal will appear at the same frequency as a component of the output, but exhibit there a certain phase shift. How much that phase shift will be we cannot say, for at any particular frequency the magnitude of the phase lag will depend not only on the time constant of the system, but also on the exact form of the system's linear response. If, for example, the system has a single-exponential response without delay, then the output will lag behind the input by no more than a quarter of a cycle. But if the system does exhibit delay, then the lag can exceed a quarter-cycle. An additional source of uncertainty attaches to the 23,000-year (but not the 40,000-year) component of the orbital input, for the phase of the precession index itself is arbitrarily defined with respect to a particular time of the year.

Although our predictive model is nonspecific, in the sense that it does not say what the shape of a particular climatic record should be, it does predict that whatever orbital-geological phase shift is observed at a particular (obliquity or precession) frequency, that shift should be constant (*19*).

Furthermore, we can assume that each climatic index reflects a response of one physical part of the climate system and is characterized by a certain time constant. Therefore, whatever phase shift is observed (at a particular frequency) between a pair of climatic indices should also be constant, and the subsystem with the larger time constant should lag the other. Because the $\delta^{18}O$ curve reflects changes in the cryosphere (a part of the climate system that must have longer time constants than the ocean), we expect that curve to lag *Ts* and percentage of *C. davisiana* at all frequencies.

Numerical procedures. Discrete spectral peaks in our geological time series have already been observed and identified as variance components related to obliquity and precession. Using a band-pass digital filter (Tukey filter), we will now extract these components from the signal and display them in the time domain (*70*). To use this phase-free filter the investigator chooses f_0, the center frequency in the band to be studied, and fixes the bandwidth by determining r, the resolution of the filter (*71*). The impact of a particular filter on the frequency domain is described by its frequency-response function, $H(f)$. We used two filters, one centered at a frequency of 0.25 cycle per 1000 years and one at 0.043 cycle per 1000 years (Fig. 7). These will be referred to as the 40K (40,000-year) and 23K (23,000-year) filters, respectively. Their bandwidths have been chosen so that the adjacent half-power points nearly coincide, and the variance in the filtered signal is approximately the same as the variance in the corresponding spectral peak.

Because filters of this type yield smooth curves no matter what data are processed (*72*), the objective in using them is simply to determine in the time domain, and for each frequency component of interest, the position of inflection points in the filtered record. Although the average interval between inflection points must match some frequency within the passband of the filter, information in the data controls the exact timing of each inflection. Phase shifts can be estimated visually by comparing two geological variables filtered at the same frequency, or by comparing an orbital curve with a geological curve filtered at the same frequency. Cross-spectral techniques are employed on unfiltered data to obtain for the frequency of interest a quantitative estimate of the average phase shift over the study interval (*73*).

Patterns in the geologic record. Two sets of curves (Fig. 8, A and C) show the results of applying filters to the ELBOW time series. The three geological curves filtered at 40K are approximately in phase throughout their length. Cross-spectral analysis shows $\delta^{18}O$ lagging *Ts* by 2000 years and percentage of *C. davisiana* by 1000 years. The data filtered at 23K show a nearly constant phase relationship between $\delta^{18}O$ and percentage of *C. davisiana* throughout the record, with $\delta^{18}O$ lagging percentage of *C. davisiana* by an average of 4000 years. After 350,000 years ago $\delta^{18}O$ systematically

Table 5. Comparison of published $\delta^{18}O$ chronologies and spectra. Dominant periods (in thousands of years) as calculated by investigators cited are correlated with spectral peaks *a*, *b*, and *c* documented in this article.

Chronological models		Correlation of dominant periods identified		
Age of 12-11 boundary ($\times 10^3$ years)	Reference	*a*	*b*	*c*
220*	Emiliani (*26*)	40		
220	van den Heuvel (*14*)†	40		13
240‡	Kemp and Eger (*16*)	~ 52	~ 27	
270§	Emiliani (*27*)	50		
270	Chappell (*20*)‖	~ 46	~ 25	
350	Imbrie and Kipp (*18*)¶	80	30	
375	Broecker and van Donk (*17*)	90		
380	Pisias (*82*)#			23
	This article:			
425	TUNE-UP age	99	42	22
440	ELBOW age	106	43	22

*Age calculated on the assumption that $\delta^{18}O$ stages reflect obliquity. †Data from Emiliani (*68*). ‡Age selected to match spectral peaks calculated from Emiliani's (*27*) $\delta^{18}O$ data with orbital frequencies. §Age calculated by extrapolation beyond a section of the curve estimated to be younger than 150,000 years by early results of the Pa/Th technique. ‖Data from Emiliani (*27*). ¶Data for $\delta^{18}O$ from Broecker and van Donk (*17*); an unconformity was later recognized in this record (*78*). #Data for $\delta^{18}O$ from Shackleton and Opdyke (*31*).

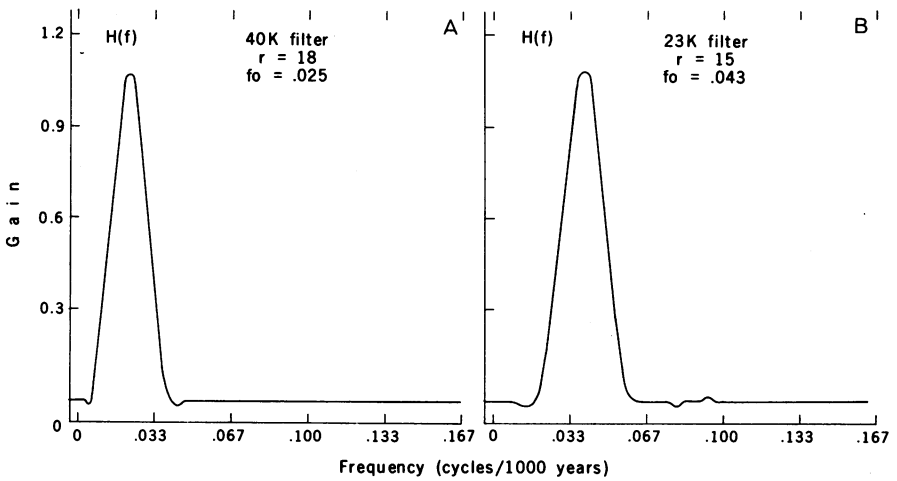

Fig. 7. Gain function for band-pass filters used to calculate curves in Figs. 8 and 9: (A) 40K filter centered on a frequency of 0.025 cycle per thousand years; (B) 23K filter centered on a frequency of 0.043 cycle per thousand years. Tukey filters were used (*70*).

lags *Ts* by an average of about 2000 years. Before that time, however, $\delta^{18}O$ and *Ts* are clearly out of phase.

The general pattern of these relationships can be observed on the stratigraphic diagrams (Figs. 2 and 3) and is independent of assumptions about chronology. Therefore, the climate changes of the two hemispheres are nearly in phase during the last 300,000 years with changes in the Southern Hemisphere ocean appearing to lead changes in the Northern Hemisphere ice sheets by up to a few thousand years. However, before 300,000 years ago *Ts* and $\delta^{18}O$ appear to be out of phase in the 23K but not the 40K frequency band.

Orbital-geologic phase relationships. Displayed on the ELBOW chronology, phase relationships between the filtered geological curves and orbital curves are systematic over the past 300,000 years (Fig. 8, A and C); that is, back to the upper part of stage 9. Over that interval, times of low temperature, high $\delta^{18}O$ ratios, and abundant *C. davisiana* follow times of low obliquity. The 40K components of the geological curves (Fig. 8C) lag obliquity by about a quarter-cycle. Measurements made at the maxima and minima of 12 obliquity half-cycles covering the interval 70,000 to 300,000 years ago show that $\delta^{18}O$, *Ts*, and percentage of *C. davisiana* lag obliquity by 9000 ± 3000, 8000 ± 3000, and 7000 ± 4000 years, respectively. Below the top of stage 9, however, the geological curves on the average lead obliquity by several thousand years.

Over the interval 0 to 150,000 years ago on the ELBOW time scale, the interval that has the most certain chronology, the 23,000-year components of the geological curves systematically lag precession by about 3000 years (Fig. 8A). However, when averaged over the interval 0 to 300,000 years they are approximately in phase with precession. Measurements made at the maxima and minima of 22 precession half-cycles covering the interval 50,000 to 300,000 years ago show that $\delta^{18}O$, *Ts*, and percentage of *C. davisiana* lag precession by 1500 ± 3500, 0 ± 3000, and −500 ± 4500 years, respectively. Times of low temperature, high $\delta^{18}O$ ratios, and abundant *C. davisiana* are associated with times of high positive values of the precession index—that is, times when the earth-sun distance in June is greater than normal. The systematic orbital-geologic phase relationships just described do not, however, exist below the 300,000-year horizon. There, a confusing pattern of leads and lags among all of the curves is displayed.

Discussion. We regard the results of the time-domain test as strong evidence of orbital control of major Pleistocene climatic changes, for the following reasons: (i) Over the past 300,000 years, each of the 40K components of the geological records exhibits a phase relationship with obliquity which is as constant as could be expected from a geological record. Monte Carlo tests we have conducted with our filters show that the degree of regularity observed would be highly unlikely as a random result. The magnitude of the phase shift (7000 to 9000 years) is less than a quarter of the cycle length. (ii) Averaged over the same interval, the 23K components of the geological curves exhibit in-phase relationships with precession which are as constant as could be expected from a geological record. Again, the observed regularity is too great to be explained as a random result. When the chronology is most accurate for the filtered record (50,000 to 150,000 years ago), the 23K components of the geological curves lag

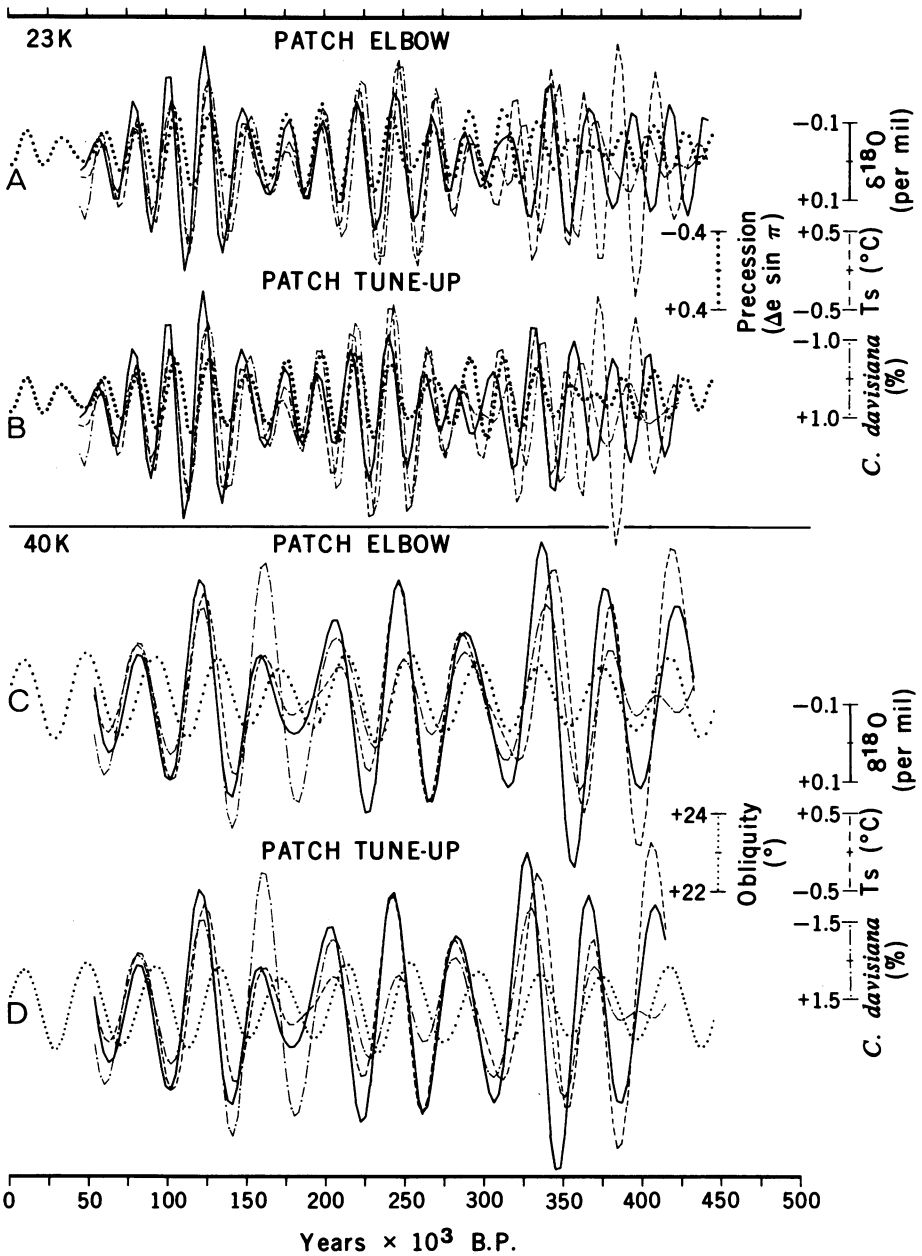

Fig. 8. Variations in obliquity, precession, and the corresponding frequency components of climate over the past 500,000 years. Orbital data are from Vernekar (*39*). Climatic curves are variations in $\delta^{18}O$, *Ts*, and percentage of *C. davisiana* plotted against alternate geological time scales (ELBOW and TUNE-UP) as defined in Table 2. The variations shown are frequency components extracted from the raw-data curves by means of digital band-pass filters (Fig. 7). The two sets of curves in (A) and (B) include the precession curve and the 23,000-year frequency components of climate based on the ELBOW (A) and TUNE-UP (B) time scales. The two sets of curves in (C) and (D) include the obliquity curve and the 40,000-year frequency components of climate based on the ELBOW (C) and TUNE-UP (D) time scales.

precession by about 3000 years. (iii) The expectation that the 23K and 40K components of the $\delta^{18}O$ curve should show a constant lag against the corresponding components of *Ts* and percentage of *C. davisiana* is confirmed by the geological record of the last 350,000 years. The out-of-phase relationship between *Ts* and $\delta^{18}O$ that appears in stage 10 and the upper part of stage 11 may be related to the low amplitudes of precession variation resulting from near-zero eccentricity at this time. This may have allowed a decoupling of *Ts* variation from precession over this short interval. (iv) The fact that the large irregularities which do occur in the observed orbital-geologic phase relationships at both frequencies are stratigraphically concentrated in the early part of the record (before 300,000 years ago) where the chronology is least accurate, rather than randomly distributed, suggests that these irregularities result from errors in the older chronology.

Implications of Test Results

Quaternary time scale. Taken together with the results of the frequency-domain test, the systematic phase relationships just described suggest that a small error occurs in the older portions of the ELBOW chronology. To explore this hypothesis we have made the minimum adjustments in the ELBOW chronology which would extend farther back in time the systematic phase relationships observed in the younger parts of the ELBOW record. These adjustments (Table 2) are easily within the absolute error of the radiometric dates on which the ELBOW time scale is based. On this revised chronology (called TUNE-UP), the age of the isotope stage 11-12 boundary is reduced by 3 percent (25,000 years), and the age of isotope stage 7-8 boundary is reduced by 2 percent (4000 years) (Table 6).

The impact of these adjustments in the time domain (Fig. 8, B and D) is to extend the systematic phase relationships previously noted with obliquity back over the whole range of the filtered record—some 425,000 years. There is also a definite improvement in the phase relationship with precession. For the $\delta^{18}O$ record, this relationship is generally regular and includes 13 cycles extending back 340,000 years. For *Ts* the relationship extends back 325,000 years, and for the percentage of *C. davisiana* back 280,000 years (with one exception near 240,000 years). We have experimented with other ages for our chronological control points and find that further adjustments result in a deterioration of the match between orbital parameters and the geological records filtered at the same frequencies (*74*). In the frequency domain, estimates for spectral peaks calculated from the TUNE-UP time series match those predicted for obliquity and precession within 1000 years (Table 5).

The 100,000-year cycle. The dominant cycles in all of our spectra (Fig. 5C and Table 4) are about 100,000 years long—an observation which merely confirms a geological opinion now widespread (*17, 18, 75–77*). Yet this cycle would not arise as a linear response of the climate system to variations in obliquity and precession. Mesolella *et al.* (*15*) and Broecker and van Donk (*17*) account for this cycle by relating it to eccentricity or to the phasing of obliquity with precession. Our data, displayed on a time scale derived without reference to eccentricity, dramatically confirm the empirical association of glacial times with intervals of low eccentricity (Fig. 9).

Because this time-domain match agrees with independent evidence in the frequency domain ($\delta^{18}O$ and *Ts* in Table 4), we conclude, as others have (*15, 18*), that the 100,000-year climate cycle is driven in some way by changes in orbital eccentricity. As before, we avoid the obligation of identifying the physical mechanism of this response, and instead characterize the behavior of the system only in general terms. Specifically, we abandon the assumption of linearity (*78*). In such a nonlinear system (*68*) there are many ways in which the modulating effect of eccentricity on the precession index could generate 100,000-year variance components in the geological record. Among these we are attracted to a hypothesis that ice sheets waste faster than they grow; that is, that two different time constants of the cryosphere's response to orbital forcing are involved. This concept (*79*) can be deduced glaciologically (*7*) or arrived at inductively

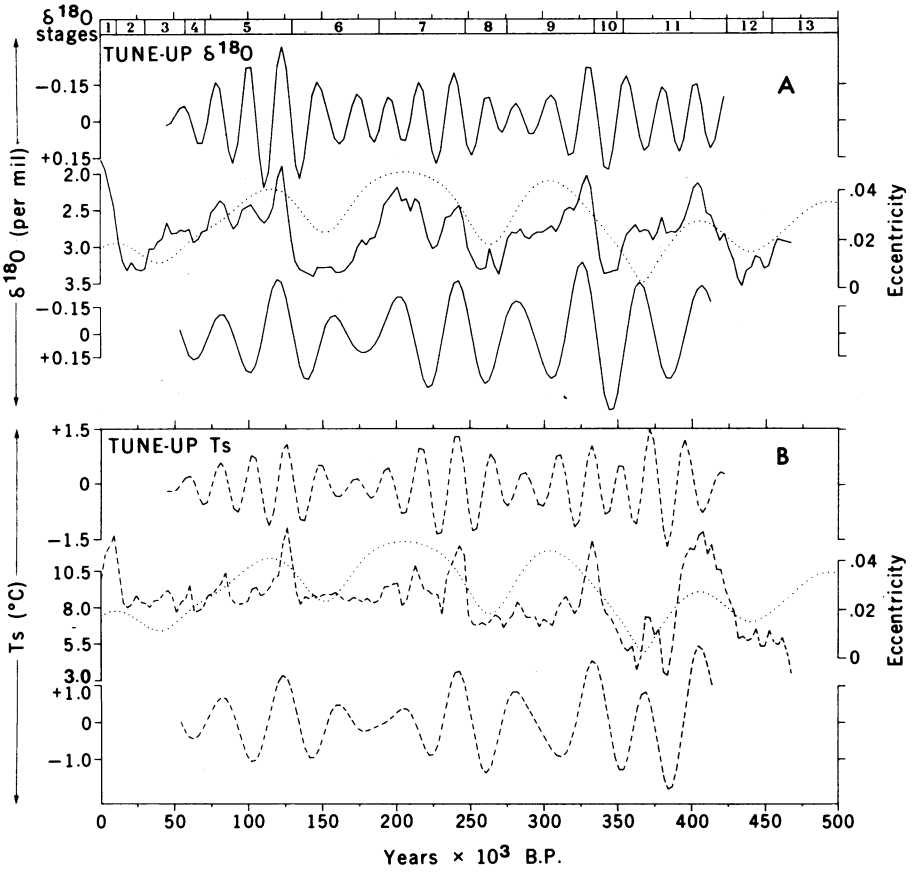

Fig. 9. Variations in eccentricity and climate over the past 500,000 years. Climatic curves are obtained from the combined (PATCH) record of two subantarctic deep-sea cores and plotted on the TUNE-UP time scale (Table 2). (A) Solid line in center shows variations in $\delta^{18}O$. Dotted line is a plot of orbital eccentricity (*39*). Upper curve is the 23,000-year frequency component extracted from $\delta^{18}O$ by a band-pass digital filter (Fig. 6). Lower curve is the 40,000-year frequency component extracted from $\delta^{18}O$ by a band-pass digital filter (Fig. 6). (B) Dashed line in center shows variations in estimated sea-surface temperature (*Ts*). Dotted line is a plot of orbital eccentricity data from Vernekar (*39*). Upper curve is the 23,000-year frequency component extracted from *Ts* by a band-pass digital filter (Fig. 6). Lower curve is the 40,000-year frequency component extracted from *Ts* by a band-pass digital filter (Fig. 6).

from the climatic record (*17*). Because the amplitude of each precession-index cycle is proportional to eccentricity, such a nonlinear response of the ice sheets would bring out the 100,000-year eccentricity signal in the geologic record by forcing the mean of the 23,000-year climatic cycle to approach values directly proportional to eccentricity.

Future climate. Having presented evidence that major changes in past climate were associated with variations in the geometry of the earth's orbit, we should be able to predict the trend of future climate. Such forecasts must be qualified in two ways. First, they apply only to the natural component of future climatic trends—and not to such anthropogenic effects as those due to the burning of fossil fuels. Second, they describe only the long-term trends, because they are linked to orbital variations with periods of 20,000 years and longer. Climatic oscillations at higher frequencies are not predicted.

One approach to forecasting the natural long-term climate trend is to estimate the time constants of response necessary to explain the observed phase relationships between orbital variation and climatic change, and then to use those time constants in an exponential-response model. When such a model is applied to Vernekar's (*39*) astronomical projections, the results indicate that the long-term trend over the next 20,000 years is toward extensive Northern Hemisphere glaciation and cooler climate (*80*).

Summary

1) Three indices of global climate have been monitored in the record of the past 450,000 years in Southern Hemisphere ocean-floor sediments.

2) Over the frequency range 10^{-4} to 10^{-5} cycle per year, climatic variance of these records is concentrated in three discrete spectral peaks at periods of 23,000, 42,000, and approximately 100,000 years. These peaks correspond to the dominant periods of the earth's solar orbit, and contain respectively about 10, 25, and 50 percent of the climatic variance.

3) The 42,000-year climatic component has the same period as variations in the obliquity of the earth's axis and retains a constant phase relationship with it.

4) The 23,000-year portion of the variance displays the same periods (about 23,000 and 19,000 years) as the quasi-periodic precession index.

5) The dominant, 100,000-year climatic component has an average period close to, and is in phase with, orbital eccentricity. Unlike the correlations between climate and the higher-frequency orbital variations (which can be explained on the assumption that the climate system responds linearly to orbital forcing), an explanation of the correlation between climate and eccentricity probably requires an assumption of nonlinearity.

6) It is concluded that changes in the earth's orbital geometry are the fundamental cause of the succession of Quaternary ice ages.

7) A model of future climate based on the observed orbital-climate relationships, but ignoring anthropogenic effects, predicts that the long-term trend over the next several thousand years is toward extensive Northern Hemisphere glaciation.

Table 6. Estimates of the ages of stage boundaries based on the TUNE-UP chronology. Except for the lowest two boundaries, the estimates are considered accurate within a range of +5000 to −1000 years (*74*).

Isotopic stage boundary	Depth in core (cm)		Age ($\times 10^3$ years)
	RC11-120	E49-18	
2-1	40		10
3-2	105		29
4-3	215		61
5-4	255		73
6-5	440	490	127
7-6	620	640	190
8-7	785	825	247
9-8	900	920	276
10-9		1115	336
11-10		1180	356
12-11		1405	~ 425
13-12		1510	~ 457

References and Notes

1. R. F. Flint, *Glacial and Quaternary Geology* (Wiley, New York, 1971); J. M. Mitchell, Jr., in *The Quaternary of the United States*, H. E. Wright, Jr., and D. G. Frey, Eds. (Princeton Univ. Press, Princeton, N.J., 1965), pp. 881–901.
2. C. Emiliani and J. Geiss, *Geol. Rundsch.* **46**, 576 (1957).
3. B. Dennison and V. N. Mansfield, *Nature (London)* **261**, 32 (1976); F. Hoyle and R. A. Lyttleton, *Proc. Cambridge Philos. Soc.* **35**, 405 (1939).
4. M. Milankovitch, *K. Serb. Akad. Beogr. Spec. Publ. 132* (1941) (translated by the Israel Program for Scientific Translations, Jerusalem, 1969).
5. J. P. Kennett and R. C. Thunell, *Science* **187**, 497 (1975).
6. G. Wollin, D. B. Ericson, W. B. F. Ryan, J. H. Foster, *Earth Planet. Sci. Lett.* **12**, 175 (1971); G. Wollin, D. B. Ericson, W. B. F. Ryan, *Nature (London)* **232**, 549 (1971).
7. J. Weertman, *J. Glaciol.* **5**, 145 (1964).
8. A. T. Wilson, *Nature (London)* **201**, 147 (1964).
9. M. Ewing and W. L. Donn, in *Polar Wandering and Continental Drift* (Society of Economic Paleontologists and Mineralogists, Tulsa, Okla., 1956), pp. 94–99.
10. G. N. Plass, *Tellus* **8**, 140 (1956).
11. R. E. Newell, *Quat. Res. (N.Y.)* **4**, 117 (1974).
12. E. N. Lorenz, *Meteorol. Monogr.* **8**, 1 (1968).
13. W. S. Broecker, *Science* **151**, 299 (1966); ———, D. L. Thurber, J. Goddard, T.-L. Ku, R. K. Matthews, K. J. Mesolella, *ibid.* **159**, 297 (1968).
14. E. P. J. van den Heuvel, *Geophys. J. R. Astron. Soc.* **11**, 323 (1966).
15. K. J. Mesolella, R. K. Matthews, W. S. Broeck er, D. L. Thurber, *J. Geol.* **77**, 250 (1969).
16. W. C. Kemp and D. T. Eger, *J. Geophys. Res.* **72**, 739 (1967).
17. W. S. Broecker and J. van Donk, *Rev. Geophys. Space Phys.* **8**, 169 (1970).
18. J. Imbrie and N. G. Kipp, in *The Late Cenozoic Glacial Ages*, K. K. Turekian, Ed. (Yale Univ. Press, New Haven, Conn., 1971), pp. 71–182.
19. G. Kukla, *Boreas* **1**, 63 (1972); *Nature (London)* **253**, 600 (1975).
20. J. Chappell, *Quat. Res. (N.Y.)* **3**, 221 (1973).
21. W. Koppen and A. Wegener, *Die Klimate der Geologischen Vorzeit* (Berlin, 1924).
22. N. J. Shackleton, *The Phanerozoic Time-Scale* (Geological Society, London, 1971), part 1, pp. 35–38.
23. A. Bloom, W. S. Broecker, J. Chappell, R. K. Matthews, K. J. Mesolella, *Quat. Res. (N.Y.)* **4**, 185 (1974).
24. T.-L. Ku, M. N. Kimmel, W. H. Easton, and T. J. O'Neil [*Science* **183**, 959 (1974)] document only the oldest of the terraces.
25. M. L. Bender, F. T. Taylor, R. K. Matthews, *Quat. Res. (N.Y.)* **3**, 142 (1973).
26. C. Emiliani, *J. Geol.* **63**, 538 (1955).
27. ———, *ibid.* **74**, 109 (1966).
28. More than a century ago, J. Croll [*Climate and Time* (Appleton, New York, 1875)] of Scotland employed the same basic strategy. He compared astronomical calculations of orbital history with the geologic record of climate, and pointed to evidence of multiple glaciations as confirming the astronomical theory of the ice ages.
29. W. L. Donn and D. M. Shaw, *Science* **157**, 722 (1966); J. M. Suarez and I. M. Held, in *Proceedings of the WMO/IAMAP Symposium on Long Term Climatic Fluctuations* (World Meteorological Organization, Geneva, Switzerland, 1975).
30. The raw data on which this study is based will be published (J. D. Hays, A. D. Vernekar, J. Imbrie, N. J. Shackleton, in preparation).
31. N. J. Shackleton and N. D. Opdyke, *Quat. Res. (N.Y.)* **3**, 39 (1973).
32. N. J. Shackleton, *Colloq. Int. CNRS* **219**, 203 (1974).
33. ———, *Nature (London)* **215**, 15 (1967); W. Dansgaard and H. Tauber, *Science* **166**, 449 (1969).
34. J. Lozano and J. D. Hays, *Geol. Soc. Am. Mem.* **145** (1976), pp. 303–336.
35. J. D. Hays, J. Lozano, N. Shackleton, G. Irving, *ibid.*, pp. 337–372.
36. M. G. Petrushevskaya, in *Biological Reports of the Soviet Antarctic Expedition (1955–1958)*, A. P. Andriyashev and P. V. Ushakov, Eds. (Leningradskoe Otdelenie, Leningrad, 1967; Israel Program for Scientific Translations, Jerusalem, 1968), p. 2.
37. J. H. Robertson, thesis, Columbia University (1975).
38. A. J. van Woerkom, *Climatic Change* (Harvard Univ. Press, Cambridge, Mass., 1953), pp. 147–157; S. G. Sharaf and N. A. Budnikova, *Tr. Inst. Teor. Astron.* **11**, 231 (1967) (translated by the Clearinghouse for Federal Scientific and Technical Information, Springfield, Va.).
39. A. D. Vernekar, *Meteorol. Monogr.* **12** (1972).
40. A. L. Berger, *Astron. Astrophys.*, in press.
41. N. J. Shackleton and N. D. Opdyke, *Geol. Soc. Am. Mem.* **145** (1976), pp. 449–464; CLIMAP Project Members, *Science* **191**, 1131 (1976).
42. D. Ninkovich and N. J. Shackleton, *Earth Planet. Sci. Lett.* **27**, 20 (1975).
43. H. Thierstein, K. Geitzenauer, B. Molfino, N. J. Shackleton, in preparation; S. Gartner, *Palaeogeogr. Palaeoclimatol. Palaeoecol.* **12**, 169 (1972).
44. J. D. Hays and N. J. Shackleton, in preparation.
45. T. Kellogg, in *Climate of the Arctic*, G. Weller and S. A. Bolliny, Eds. (Geophysical Institute, Univ. of Alaska, Fairbanks, 1975), pp. 3–36; *Geol. Soc. Am. Mem.* **145** (1976), pp. 77–110.
46. J. D. Hays and D. Ninkovich, *Geol. Soc. Am. Mem.* **126** (1970), p. 263; J. D. Hays and N. Opdyke, *Science* **158**, 1001 (1967).
47. We have used only those ages for the stage 12-11 boundary based on interpolations between the core top and the Brunhes-Matuyama magnetic reversal. Although Hays *et al.* [J. D. Hays, T. Saito, N. D. Opdyke, L. H. Burckle, *Geol. Soc. Am. Bull.* **80**, 1481 (1969)] estimated the time of extinction of *Stylatractus universus* by this method and obtained an estimate of 341,000

years, Shackleton and Opdyke (*31*) argued convincingly that this estimate was too young, because of sedimentation rate changes between the lower and upper Brunhes magnetic series. We have not used estimates based on Io/Th techniques because we believe the intrinsic inaccuracy of these estimates is large.
48. C. Emiliani and N. J. Shackleton, *Science* **183**, 511 (1974).
49. E. Rona and C. Emiliani, *ibid.* **163**, 66 (1969).
50. H. H. Veeh and J. M. A. Chappell, *ibid.* **167**, 862 (1970).
51. T.-L. Ku and W. S. Broecker, *ibid.* **151**, 448 (1966).
52. C. Sancetta, J. Imbrie, N. G. Kipp, *Quat. Res. (N.Y.)* **3**, 110 (1973).
53. L. A. Zadeh and C. A. Desoer, *Linear System Theory* (McGraw-Hill, New York, 1963), p. 628.
54. In this section of the article we have benefited from discussions with W. A. Wolovich.
55. G. M. Jenkins and D. G. Watts, *Spectral Analysis and Its Applications* (Holden-Day, San Francisco, 1968).
56. R. B. Blackman and J. W. Tukey, *The Measurement of Power Spectra from the Point of View of Communication Engineering* (Dover, New York, 1958), p. 190.
57. The procedures are as follows: (i) Selection of an absolute chronology. For astronomical variables, we adopt the chronology of Vernekar (*39*). For geological variables, we use our chronological models discussed above. (ii) Calculation of a time series. A uniform sampling interval (Δt) approximately equal to the average interval between sample points is chosen (in this study, 3000 years), and a time series of n values is calculated by linear interpolation. For the PATCH time series, n ranges from 157 to 163 according to the chronology used. (iii) Detrending. Any long-term trend is removed by calculating residuals from linear regression. (iv) Prewhitening. If the spectrum is dominated by low-frequency components the signal may be prewhitened by means of a first-difference filter in which the intensity of the prewhitening is controlled by a constant, C. In our study, $C = 0.998$ (*56*). (v) Lagging. The number of lags (m) to be used in the next step is chosen according to the bandwidth (amount of detail) desired in the estimated spectrum. (vi) Calculation of autocovariance function. The covariance between the original time series and each of m lagged versions is calculated. (vii) Smoothing. The autocovariance function, smoothed by a Hamming lag window, yields a bandwidth of approximately $1.25/m\Delta t$ cycles per thousand years. To establish the general trend of the spectrum, we fix m as 8; the resulting spectrum has high accuracy but low resolution. For more detail, m is fixed at 40 to 50, depending on n. (viii) Spectral estimation. Variance contributions to each of $m + 1$ frequency bands are calculated by a Fourier transform of the smoothed autocovariance function. The resulting spectrum has a frequency range from zero to the Nyquist frequency ($fn = 1/2\Delta t$), the highest frequency that can be determined with a given Δt. Frequencies in cycles per thousand years are plotted on a linear scale; a reciprocal scale indicates cycle length in thousands of years. (ix) Scaling. The initial estimates of an unprewhitened signal specify variance ("power") as a function of frequency, that is, $P(f)$. For prewhitened spectra, the corresponding symbol is $Pc(f)$. To simplify the use of confidence intervals, variance is expressed on a log scale. To facilitate the comparison of spectra calculated from variables with different scales, values of $P(f)$ are rescaled as $\bar{R}(f)$ so that the area under the curve equals unity. (x) Statistical evaluation. A one-sided confidence interval attached to each estimate in the high-resolution spectrum is calculated from the chi-square distribution, using $2n/m$ degrees of freedom, and expressed on a log scale (*55*, *56*). Calculations in steps iii through viii were carried out with a BMDO2T program (*58*) modified by Y. Yeracaris to avoid recoloring the spectrum when the prewhitening option is used.
58. W. J. Dixon, Ed., *BMD Biomedical Computer Programs* (Los Angeles School of Medicine, Univ. of California, Los Angeles, 1965), p. 620.
59. A. L. Berger [in *Symposium on Long-Term Climatic Fluctuations*, Norwich, August, 1975 (World Meteorological Organization, Geneva, 1975), pp. 65–72] concludes that variations in eccentricity are positively correlated with planetary insolation receipt, and that, although small, this effect might be climatically significant.
60. Changes in Π reflect the interaction of precession with the changing orientation of the orbital ellipse.
61. This interpretation of the precession curve, due to Broecker and van Donk (*17*), was confirmed by A. L. Berger (personal communication) as accurate to the first order of the earth's eccentricity.
62. Digital data were provided by A. D. Vernekar.
63. We have estimated astronomical frequencies by two methods: averaging the number of peaks in the time domain, and spectral analysis (Tables 3 and 4). The averaging gives satisfactory results for simple sinusoidal curves such as obliquity, but cannot resolve the component frequencies in more complex precession, insolation, or climate curves. For uniformity, spectral estimates are used exclusively in this article.
64. Higher-resolution spectra of much longer eccentricity records actually have two discrete peaks (corresponding to periods of 96,000 and 125,000 years).
65. Discussions with J. W. Tukey were helpful in framing statistical hypotheses and in properly prewhitening the signals.
66. Questions of sampling variance apart, there are two ways in which our results might be artifacts of procedure. First, the *b* and *c* peaks could be aliases of cycles present in the cores but not visible in our data because their frequencies are higher than the Nyquist frequency. However, the mixing of deep-sea sediments by bottom-living animals rules out the possibility that signals with sufficient power at these frequencies could remain in the record. Second, a significant part of the variance in the data for $\delta^{18}O$ and particularly for *Ts* has the form of a Dirac comb—that is, has equally spaced spikes (Figs. 2 and 3). As the Fourier transform of a comb yields a comblike spectrum with frequencies that are harmonics of the fundamental, it might be supposed that our *b* and *c* peaks (42,000, 24,000, and 19,500 years) could be statistically blurred versions of the third, fifth, and sixth harmonics of a fundamental 122,000-year cycle (~ 41,000, ~ 24,000, and ~ 20,000 years). But several arguments can be advanced which eliminate this possibility: (i) No discrete spectral peaks occur at frequencies corresponding to the second and fourth harmonics (61,000 and ~ 30,000 years) of the presumed fundamental. (ii) The dominant frequencies of peaks *b* and *c* are not harmonics of the dominant cycles we estimate in *a* (94,000 years for *Ts* and 106,000 years for $\delta^{18}O$). (iii) Although the percentage of *C. davisiana a* peak actually has a dominant period near 122,000 years, and its 42,000-year spectral peak is strongly developed, this time series does not approach a Dirac comb.
67. This method [R. T. Lacoss, *Geophysica* **36**, 661 (1971)] was applied to our data by T. E. Landers, Lincoln Laboratory, Massachusetts Institute of Technology.
68. H. S. Tsien, *Engineering Cybernetics* (McGraw-Hill, New York, 1952), p. 164.
69. C. Emiliani, *Ann. N.Y. Acad. Sci.* **95**, 521 (1961).
70. N. R. Goodman, *J. Franklin Inst.* **270**, 437 (1960).
71. The larger the value of r, the narrower the passband. Because the filter is an array of $2r + 1$ weights for a moving average applied in the time domain, r data points are lost at the end of the filtered signal. All of our filter calculations were carried out with a BMDO1T program (*58*).
72. E. Slutsky, *Econometria* **5**, 105 (1937).
73. Cross-spectral techniques (*55*) were first applied to deep-sea cores by Moore *et al.* [T. C. Moore, Jr., N. Pisias, G. R. Heath, in *The Fate of Fossil Fuel CO_2* (Plenum, New York, in press)].
74. In arriving at the TUNE-UP chronology, we first experimented with ages of the stage 12-11 boundary ranging from 380,000 to 440,000 years ago, while retaining the stage 6-5 and younger ELBOW control points (Table 2). The phase coherences between the orbital and filtered geological signals reached a maximum in these experiments when the 12-11 boundary was fixed at 425,000 years. With that boundary determined, we then experimented with different ages of the 8-7 and 6-5 boundaries to arrive at the TUNE-UP chronology. To evaluate the uncertainty of this chronology over the interval 50,000 to 350,000 years ago (where we can check phase coherence at both frequencies) we next conducted trials in which the three oldest TUNE-UP control points were all shifted by the same experimental interval, while holding constant the 9400-year level dated by carbon-14 and the zero-age core top. With a shift of either plus or minus 22,000 years (that is, an interval equal to an average precession cycle and approximately equal to half an obliquity cycle), the phase coherences are drastically disturbed in the younger part of the record. A final experimental series in which the three oldest TUNE-UP control points were shifted together over a range of ± 6000 years shows that the only chronologies worth serious consideration (under the hypothesis of phase coherence at the frequencies of obliquity and precession) show deviations from the TUNE-UP values ranging between +5000 and −1000 years, with the optimum phase matches from 50,000 to 350,000 years ago being very close to that fixed by the TUNE-UP chronology (Table 2).
75. G. Kukla, *Geol. Foeren. Stockholm Foerh.* **92**, 148 (1970).
76. W. F. Ruddiman and A. McIntyre, *Geol. Soc. Am. Mem.* **145** (1976), pp. 111–146.
77. U.S. Committee for the Global Atmospheric Research Program, National Research Council, *Understanding Climatic Change, A Program for Action* (National Academy of Sciences, Washington, D.C., 1975), figure A-14.
78. J. Imbrie, J. van Donk, N. G. Kipp, *Quat. Res. (N.Y.)* **3**, 10 (1973).
79. N. Calder, *Nature (London)* **252**, 216 (1974).
80. J. Imbrie and J. Z. Imbrie, in preparation.
81. J. Hülsemann, *J. Sediment. Petrol.* **36**, 622 (1966).
82. N. G. Pisias, *Geol. Soc. Am. Mem.* **145** (1976), pp. 375–392.
83. Supported by NSF IDOE grants IDO 71-04204 and OCE 75-19627 to Lamont-Doherty Geological Observatory of Columbia University; NSF grant OCD 75-14934 to Brown University; and NERC grant GR 3/1762 to Cambridge University, England. We are grateful to those who materially contributed to this article in the following ways: data generation, G. Irving, K. Jare (radiolarian counts), M. A. Hall (operation of V.G. Micromass mass spectrometer), A. Vernekar (orbital and insolation data in digital form), and A. L. Berger (digital data on seasonal insolations); data processing, Y. Yeracaris, J. Morley, N. Kipp, D. Kirkpatrick, and J. Z. Imbrie; production of manuscript, R. M. Cline, M. Perry, and R. Mellor. We are also grateful to all those who freely contributed their ideas and critically read the manuscript; in particular we wish to thank J. M. Mitchell, Jr., A. Cox, T. Hughes, J. W. Tukey, G. Kukla, A. Berger, and S. Sachs. We are grateful to all our CLIMAP colleagues who encouraged and criticized this work during the past 2 years. This article is Lamont-Doherty Geological Observatory Contribution 2434.